

## Convergent Preparation and Photophysical Characterization of Dimaleimide Dansyl Fluorogens: Elucidation of the Maleimide Fluorescence Quenching Mechanism

Julia Guy,<sup>†</sup> Karine Caron,<sup>†</sup> Stéphane Dufresne,<sup>†</sup> Stephen W. Michnick,<sup>‡</sup>  
W.G. Skene,<sup>\*†</sup> and Jeffrey W. Keillor<sup>\*†,‡</sup>

Contribution from the Department of Chemistry and Department of Biochemistry, Université de Montréal, C.P. 6128, Succursale centre-ville, Montréal, Québec, H3C 3J7, Canada

Received May 26, 2007; E-mail: w.skene@umontreal.ca; jw.keillor@umontreal.ca

**Abstract:** Dimaleimide fluorogens are being developed for application to fluorescent protein labeling. In this method, fluorophores bearing two maleimide quenching groups do not fluoresce until both maleimide groups have undergone thiol addition reactions with the Cys residues of the target protein sequence [*J. Am. Chem. Soc.* **2005**, *127*, 559–566]. In this work, a new convergent synthetic route was developed that would allow any fluorophore to be attached via a linker to a dimaleimide moiety in a modular fashion. Series of dimaleimide and dansyl derivatives were thus prepared conveniently and used to elucidate the mechanism of maleimide quenching. Intersystem crossing was ruled out as a potential quenching pathway, based on the absence of a detectable triplet intermediate by laser flash photolysis. Stern–Volmer rate constants were measured with exogenous dimaleimide quenchers and found to be close to the diffusion-controlled limits, consistent with electron transfer being thermodynamically favorable. The thermodynamic feasibility of the photoinduced electron transfer (PET) quenching mechanism was verified by cyclic voltammetry. The redox potentials measured for dansyl and maleimide confirm that electron transfer from the dansyl excited state to a pendant maleimide group is exergonic and is responsible for fluorescence quenching of the fluorogens studied herein. Taking this PET quenching mechanism into account, future fluorogenic protein labeling agents will be designed with spacers of variable length and rigidity to probe the structure–property PET efficiency relationship.

### Introduction

Categorizing the huge number of gene products discovered in this post-genomic era remains a monumental task. New complementary protein labeling techniques are required to accelerate and facilitate the process. The fluorescent labeling of proteins has proven to be a powerful approach for following the dynamic process of their synthesis and degradation, in addition to determining their localization and protein–protein interactions. Many labeling techniques have been developed that are based on the reaction of fluorescent dyes, through succinimidyl ester or maleimide functional groups, with primary amines or thiol groups exposed on the surface of a protein.<sup>1–3</sup> However, the frequency of such functional groups on protein surfaces renders these labeling techniques nonspecific. One broadly applied method for labeling specific target proteins is their genetic fusion to fluorescent proteins such as jellyfish green fluorescent protein (GFP). This approach has been used to study individual protein dynamics in living cells<sup>4</sup> and to determine

the cellular localization of proteins at a whole genome scale,<sup>5</sup> but there remain some limitations for this method. For GFP to function as a fluorophore, it must be properly folded into its 11-stranded  $\beta$ -barrel structure; however, maturation into a soluble, fluorescent protein is not spontaneous and may be problematic, especially at or above room temperature.<sup>6</sup> GFP fluorescence is also sensitive to the environment of its fusion with test proteins and can be difficult to distinguish from the autofluorescent background of living cells. GFP variants have been produced through protein engineering that are able to overcome some of these limitations, but the steric bulk and metabolic stability of a 27 kDa  $\beta$ -barrel protein still represents the potential for significant perturbation of the dynamics and localization of test proteins.<sup>4,6</sup>

Alternative protein labeling strategies have been developed that address the steric bulk and stability problems. For example, Tsien and co-workers have elaborated on a method<sup>7</sup> that makes use of a short peptide sequence, optimized to form a  $\beta$ -turn motif,<sup>8</sup> that contains four Cys residues positioned to allow their reaction with a biarsenical fluorogenic compound. The resulting

<sup>†</sup> Department of Chemistry.

<sup>‡</sup> Department of Biochemistry.

(1) For example, see Haughland, R.P. In *Handbook of Fluorescent Probes and Research Chemicals*, 5th ed.; Molecular Probes: Eugene, OR, 1992.

(2) Sipple, T. O. *J. Histochem. Cytochem.* **1981**, *29*, 314.

(3) Corrie, J. E. T. *J. Chem. Soc., Perkin Trans. 1* **1994**, 2975.

(4) For a recent review, see: Zhang, J.; Campbell, R. E.; Ting, A. Y.; Tsien, R. Y. *Nat. Rev. Mol. Cell Biol.* **2002**, *3*, 906.

(5) Huh, W.-K.; Falvo, J. V.; Gerke, L. C.; Carroll, A. S.; Howson, R. W.; Weissman, J. S.; O'Shea, E. K. *Nature* **2003**, *425*, 686.

(6) Tsien, R. Y. *Annu. Rev. Biochem.* **1998**, *67*, 509.

(7) Griffin, B. A.; Adams, S. R.; Tsien, R. Y. *Science* **1998**, *281*, 269.

(8) Adams, S. R.; Campbell, R. E.; Gross, L. A.; Martin, B. R.; Walkup, G. K.; Yao, Y.; Llopis, J.; Tsien, R. Y. *J. Am. Chem. Soc.* **2002**, *124*, 6063.

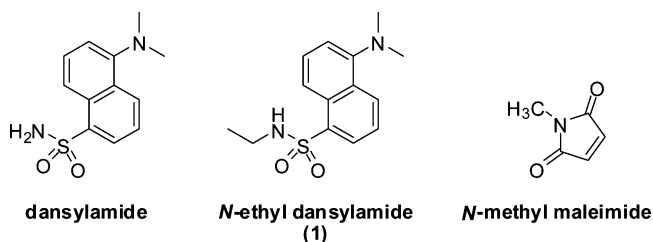
biarsenical protein adduct is far more fluorescent than the initial fluorogen. The probe peptide sequence is small (only 16 aa in its typical application<sup>8</sup>), minimizing perturbation of the target protein, and presents a hexapeptide 4-Cys motif (CCPGCC) that confers enough specificity for the biarsenical fluorogen that it may be used *in vivo*.<sup>8</sup> The toxicity of the arsenic derivatives is the most obvious disadvantage of this method, although protocols have been developed<sup>9</sup> for the administration of antidotes that render the method broadly applicable. Methods that do not rely on such toxic metals would offer a complementary alternative.

Maleimides are known to quench fluorescence in their conjugated form.<sup>10</sup> The conjugated C=C double bond of a maleimide group is also known to undergo addition reactions with significant selectivity for thiols. After this addition reaction, the resulting thioalkyl succinimide groups no longer exhibit a strong quench effect. Naphthopyranone,<sup>11,12</sup> phthalimide,<sup>13</sup> pyrene,<sup>14</sup> and aminophenoxazone<sup>15</sup> derivatives bearing a maleimide group have thus been shown to undergo a dramatic increase in fluorescence upon their reaction with thiols. We have recently synthesized and characterized a first generation of fluorogens that contain two maleimide groups, reasoning that their latent fluorescence would only be realized upon its reaction with 2 equiv of thiol.<sup>16–18</sup> Furthermore, these maleimide groups were separated by a precise distance on the fluorescent core, allowing the fluorogens to react rapidly and specifically with compounds presenting two sulfhydryl groups separated by the appropriate distance. This was demonstrated for a dicysteine mutant of the helical protein Fos, which bodes well for the application of dimaleimide fluorogens to the labeling of proteins bearing a short helical target sequence.

To date, the maleimide fluorescence quenching mechanism has only been speculated. In fact, relatively few studies have examined the mechanism of fluorescence quenching by maleimides, and their conclusions differ greatly, ranging from photoinduced electron transfer (PET)<sup>14</sup> to rearrangement of molecular orbitals.<sup>19,20</sup> Since these conclusions were indirectly derived without direct evidence for either mechanism, the subsequent refinement of a method for labeling proteins using dimaleimide fluorogens requires an understanding of the photophysical behavior of the maleimide group. Comprehension of the mechanism of the quench process, before and after thiol addition, is critical for the rational design of successive generations of fluorogens that will, ideally, fluoresce very weakly until their intense fluorescence is restored upon reaction with a dicysteine target sequence.

A new modular synthetic route was therefore developed to prepare a series of fluorophore-dimaleimides providing direct

Chart 1



evidence to unequivocally establish the fluorescence quenching mechanism. Our devised route allows a variety of dimaleimide moieties to be attached via a variable linker moiety to a number of different fluorophores. This convergent synthetic route permitted the facile preparation of a series of derivatives of dimaleimide dansyl fluorogens. These derivatives enabled us to unequivocally elucidate the mechanism of maleimide quenching, including the intermolecular quenching of dansylamide and *N*-ethyl dansylamide (**1**) by *N*-methylmaleimide (see Chart 1). The application of this information in the design of successive generations of fluorogenic protein labeling agents is also discussed herein.

## Experimental Section

**Generalities.** All starting materials were purchased from Sigma Aldrich and used without further purification. Solvents were dried using GlassContour System (Irvine, CA) columns. Reactions requiring anhydrous conditions were carried out under a dry nitrogen atmosphere employing conventional benchtop techniques. <sup>13</sup>C and <sup>1</sup>H NMR spectra were recorded on AMXR400 and AMX300 spectrometers and were referenced to the residual proton or <sup>13</sup>C signal of the solvent. Mass spectra were determined by FAB+ ionization on an AutoSpec Q spectrometer at the Regional Mass Spectrometry Centre at the Université de Montréal. Melting points (uncorrected) were determined on a Unimelt Tomas-Hoover melting point apparatus.

**Synthesis N-Ethyl-[1-(dimethylamino)-5-naphthalene]sulfonamide (1):** A solution of dansyl chloride (300 mg; 1.12 mmol; 1 equiv) in dry CH<sub>2</sub>Cl<sub>2</sub> (20 mL) was treated with ethylamine in THF (0.72 mL; 1.45 mmol; 1.3 equiv) followed by Et<sub>3</sub>N (0.31 mL; 2.22 mmol; 2 equiv) under a nitrogen atmosphere. After the mixture was stirred for 2.5 h at room temperature, the solvent was removed *in vacuo* and the crude product was purified by flash chromatography on silica gel (100% CHCl<sub>3</sub>), leading to the desired product **1** (120 mg; 0.43 mmol; 39%) as a green solid. Mp: 134–136 °C (lit.:<sup>21</sup> 126 °C). <sup>1</sup>H NMR (CDCl<sub>3</sub>): 8.59 (d, *J* = 8.5 Hz, 1H), 8.33 (d, *J* = 8.7 Hz, 1H), 8.29 (dd, *J* = 7.3 Hz, *J* = 1.2 Hz, 1H), 7.64–7.54 (m, 2H), 7.23 (d, *J* = 7.4 Hz, 1H), 4.70 (t, *J* = 6.0 Hz, 1H, NH), 3.04–2.99 (m, 2H), 2.94 (s, 6H), 1.08 (t, *J* = 7.2 Hz, 3H). <sup>13</sup>C NMR (CDCl<sub>3</sub>): 152.8, 135.5, 131.3, 130.7, 130.6, 130.5, 129.3, 124.1, 119.6, 116.0, 46.3, 39.2, 16.0. MS: [M + H]<sup>+</sup>: 279.12.

**3,5-Dimaleimidobenzoic Acid (2):** A solution of 3,5-diaminobenzoic acid (200 mg; 1.31 mmol; 1 equiv) and maleic anhydride (385 mg; 3.93 mmol; 3 equiv) in CHCl<sub>3</sub> (12 mL) was heated to reflux for 20 h. The resulting yellow precipitate was filtered, and acetic anhydride (10 mL) and sodium acetate (35.1 mg; 0.52 mmol; 0.4 equiv) were added. The mixture was heated for another 1.5 h at 100 °C. The resulting clear solution was poured on ice, and cold water (30 mL) was added. A precipitate was formed after 10 min, and the mixture was vigorously stirred for an additional hour. The precipitate was filtered and washed with cold distilled water (100 mL) to give acid **2** (297 mg; 0.95 mmol) as a beige solid in 72% yield. Mp: >180 °C. <sup>1</sup>H NMR (DMSO-*d*<sub>6</sub>):

- (9) Griffin, B. A.; Adams, S. R.; Jones, J.; Tsien, R. Y. *Methods Enzymol.* **2000**, 327, 565.  
 (10) Kokotos, G.; Tzougrakic, C. *J. Heterocycl. Chem.* **1986**, 23, 87.  
 (11) Yang, J.-R.; Langmuir, M. E. *J. Heterocycl. Chem.* **1991**, 28, 1177.  
 (12) Langmuir, M. E.; Yang, J.-R.; Moussa, A. M.; Laura, R.; LeCompte, K. A. *Tetrahedron Lett.* **1995**, 36, 3989.  
 (13) Corrie, J.E.T. *J. Chem. Soc., Perkin Trans. I* **1994**, 2975.  
 (14) de Silva, A. P.; Gunaratne, N.; Gunnlaugsson, T. *Tetrahedron* **1991**, 39, 5077.  
 (15) Cohen, B. E.; Pralle, A.; Yao, X.; Swaminath, G.; Gandhi, C. S.; Jan, Y. N.; Kobilka, B. K.; Isacoff, E. Y.; Jan, L. Y. *Proc. Natl. Acad. Sci. U.S.A.* **2005**, 102, 965.  
 (16) Girouard, S. M.Sc. thesis, Université de Montréal, 2000.  
 (17) Houle, M.-H. M.Sc. thesis, Université de Montréal, 2002.  
 (18) Girouard, S.; Houle, M.-H.; Grandbois, A.; Keillor, J. W.; Michnick, S. W. *J. Am. Chem. Soc.* **2005**, 127, 559.  
 (19) Wu, C.-W.; Yarbrough, L. R.; Wu, F. Y.-H. *Biochemistry* **1976**, 15, 2863.

- (20) Kanaoka, Y.; Machida, M.; Ando, K.; Sekine, T. *Biochim. Biophys. Acta* **1970**, 207, 269.  
 (21) Kallmayer, H.-J.; Schwarz, P. *Pharmazie* **1989**, 44, 119.

7.96 (d,  $J = 2$  Hz, 2H), 7.64 (t,  $J = 2$  Hz, 1H), 7.23 (s, 4H).  $^{13}\text{C}$  NMR (DMSO- $d_6$ ): 169.7, 166.0, 134.9, 132.4, 132.2, 128.6, 126.4. MS:  $[\text{M} + \text{H}]^+$ : 313.05.

**3,5-Dimaleimidobenzoyl Chloride (3):** A stirred suspension of acid **1** (402 mg; 1.29 mmol; 1 equiv) in thionyl chloride (10 mL) was heated to reflux until a clear solution had formed, after which the excess  $\text{SOCl}_2$  was evaporated *in vacuo* and the resulting solid was dried under vacuum to obtain 400 mg (1.21 mmol; 94%) of **3** as a beige solid which was used without further purification. Mp:  $>180$  °C.  $^1\text{H}$  NMR (DMSO- $d_6$ ): 7.96 (d,  $J = 2$  Hz, 2H), 7.64 (t,  $J = 2$  Hz, 1H), 7.22 (s, 4H).  $^{13}\text{C}$  NMR (DMSO- $d_6$ ): 169.7, 166.0, 143.8, 134.9, 132.4, 132.1, 126.4. MS:  $[\text{M} + \text{Na}]^+$ : 352.99.

**2-tert-Butoxycarbonylaminoethylamine (4):** A solution of di-*tert*-butyldicarbonate (3.26 g; 15 mmol; 1 equiv) in  $\text{CH}_2\text{Cl}_2$  (30 mL) was added dropwise to a solution of ethylenediamine (10 mL; 150 mmol; 10 equiv) in  $\text{CH}_2\text{Cl}_2$ . The resulting reaction mixture was stirred at room temperature for 20 h. The  $\text{CH}_2\text{Cl}_2$  was then removed *in vacuo*. The residue was taken up in EtOAc (30 mL), washed with a saturated solution of  $\text{Na}_2\text{CO}_3$  (2  $\times$  20 mL), dried over  $\text{MgSO}_4$ , and concentrated *in vacuo* to furnish the desired product **4** (2.1 g; 13.4 mmol) as a white foam with 89%.  $^1\text{H}$  NMR ( $\text{CDCl}_3$ ): 5.09 (bs, 1H,  $\text{NH}_2$ ), 3.13–3.08 (m, 3H), 2.74 (t,  $J = 5.8$  Hz,  $J_2 = 5.8$  Hz, 2H), 1.38 (s, 9H).  $^{13}\text{C}$  NMR ( $\text{CDCl}_3$ ): 156.3, 79.2, 43.3, 41.8, 28.4. MS:  $[\text{M} + \text{H}]^+$ : 161.13.

**N-8-tert-Butoxycarbonylamino-3,6-dioxaoctylamine (5):** A solution of di-*tert*-butyldicarbonate (1.1 g; 5.00 mmol; 1 equiv) in  $\text{CH}_2\text{Cl}_2$  (5 mL) was added dropwise to a solution of 2,2'-(ethylenedioxy)bis(ethylamine) (7.32 mL; 50.0 mmol; 10 equiv) in  $\text{CH}_2\text{Cl}_2$  (15 mL). The resulting reaction mixture was stirred at room temperature for 21 h. The  $\text{CH}_2\text{Cl}_2$  was then removed *in vacuo*. The white foam was taken up in EtOAc (125 mL), washed with a saturated solution of  $\text{Na}_2\text{CO}_3$  (3  $\times$  50 mL), dried over  $\text{MgSO}_4$ , and concentrated *in vacuo* to furnish the desired monoprotected amine **5** (1.0 g; 4.05 mmol) as a colorless oil in 81% yield.  $^1\text{H}$  NMR ( $\text{CDCl}_3$ ): 5.26 (bs, 1H,  $\text{NH}$ ), 3.60–3.58 (m, 4H), 3.52–3.48 (m, 4H), 3.37–3.28 (m, 2H), 2.87 (bs, 2H,  $\text{NH}_2$ ), 1.97–1.94 (m, 2H), 1.42 (s, 9H).  $^{13}\text{C}$  NMR ( $\text{CDCl}_3$ ): 156.9, 79.9, 74.1, 71.1, 71.0, 42.5, 41.1, 29.2. MS:  $[\text{M} + \text{H}]^+$ : 249.18.

**N-[2-tert-Butoxycarbonylaminoethyl]-3,5-dimaleimidobenzamide (6):** To a solution of compound **3** (423 mg; 1.28 mmol; 1 equiv) in dry  $\text{CH}_2\text{Cl}_2$  (30 mL) were added amine **4** (272 mg; 1.70 mmol; 1.3 equiv) in  $\text{CH}_2\text{Cl}_2$  (10 mL) and 0.37 mL of triethylamine (2.62 mmol; 2 equiv) under a nitrogen atmosphere. After the mixture was stirred at room temperature for 2.5 h, the organic layer was washed with a saturated solution of  $\text{NaHCO}_3$  (4  $\times$  30 mL), dried over  $\text{MgSO}_4$ , and concentrated *in vacuo* to give the desired compound **6** (557.3 mg; 1.23 mmol) as a brown solid in 94% yield. Mp:  $>180$  °C.  $^1\text{H}$  NMR ( $\text{CDCl}_3$ ): 7.83 (d,  $J = 1.5$  Hz, 2H), 7.58 (t,  $J = 1.8$  Hz, 1H), 7.44 (bs, 1H), 6.88 (s, 4H), 5.13 (bt,  $J = 5.6$  Hz, 1H,  $\text{NH}$ ), 3.58–3.53 (m, 2H), 3.40–3.38 (m, 2H), 1.39 (s, 9H).  $^{13}\text{C}$  NMR ( $\text{CDCl}_3$ ): 168.9, 166.0, 157.4, 136.1, 134.4, 132.2, 125.4, 123.5, 79.8, 41.9, 40.1, 28.4. MS:  $[\text{M} + \text{H}]^+$ : 455.16.

**N-(2-Aminoethyl)-3,5-dimaleimidobenzamide (7):** Under a nitrogen atmosphere at room temperature was combined amide **6** (557.3 mg; 1.23 mmol; 1 equiv) and trifluoroacetic acid (20 mL). The reaction mixture was stirred for 1.5 h, concentrated *in vacuo*, triturated with  $\text{Et}_2\text{O}$  (20 mL), filtered, and dried to afford **7** quantitatively as its trifluoroacetate salt (437 mg; 1.23 mmol).  $^1\text{H}$  NMR ( $\text{CD}_3\text{OD}$ ): 7.77 (d,  $J = 1.8$  Hz, 2H), 7.55 (t,  $J = 1.8$  Hz, 1H), 6.98 (s, 4H), 3.64 (t,  $J = 5.8$  Hz, 2H), 3.22 (bs, 2H,  $\text{NH}_2$ ), 3.17 (t,  $J = 5.8$  Hz, 2H).  $^{13}\text{C}$  NMR ( $\text{CD}_3\text{OD}$ ): 171.7, 165.9, 136.2, 135.7, 133.2, 128.5, 125.5, 40.2, 38.5. MS:  $[\text{M} + \text{H}]^+$ : 355.10.

**N-[2-(1-(Dimethylamino)-5-naphthalene-sulfonyl)aminoethyl]-3,5-dimaleimidobenzamide (8):** To a solution of amine **7** (205.9 mg; 0.44 mmol; 1 equiv) in dry  $\text{CH}_3\text{CN}$  (30 mL) dansyl chloride (155 mg; 0.57 mmol; 1.3 equiv) in dry  $\text{CH}_3\text{CN}$  (10 mL) was added followed by  $\text{Et}_3\text{N}$  (0.13 mL; 0.88 mmol; 2 equiv) under a nitrogen atmosphere and stirred at room temperature overnight. The solvent was removed *in*

*vacuo*, and the crude product was triturated with  $\text{CH}_2\text{Cl}_2$  and filtered to yield 201.1 mg (0.34 mmol; 78%) of the desired product **8** as a white powder. Mp: 161–163 °C.  $^1\text{H}$  NMR (DMSO- $d_6$ ): 8.58 (bt,  $J = 5.5$  Hz, 1H,  $\text{NH}$ ), 8.43 (d,  $J = 8.6$  Hz, 2H), 8.28 (d,  $J = 8.7$  Hz, 1H), 8.09 (dd,  $J = 7.3$  Hz,  $J = 1.2$  Hz, 1H), 7.94–7.90 (m, 1H), 7.79 (d,  $J = 1.9$  Hz, 2H), 7.54–7.45 (m, 3H), 7.15 (d,  $J = 7.7$  Hz, 1H), 7.07 (s, 4H), 3.34–3.30 (m, 2H), 2.96–2.93 (m, 2H), 2.83 (s, 6H).  $^{13}\text{C}$  NMR (DMSO- $d_6$ ): 170.9, 165.8, 152.6, 137.0, 136.7, 136.1, 133.3, 130.8, 130.3, 130.2, 129.6, 129.2, 128.9, 126.2, 124.9, 120.2, 116.4, 47.0, 46.3, 42.9. MS:  $[\text{M} + \text{H}]^+$ : 588.15.

**N-[8-tert-Butoxycarbonylamino-3,6-dioxaoctyl]-1-dimethylamino-5-naphthalene-sulfonamide (9):** To a solution of dansyl chloride (405 mg; 1.50 mmol; 1 equiv) in dry  $\text{CH}_2\text{Cl}_2$  (15 mL) was added a solution of amine **5** (447 mg; 1.80 mmol; 1.2 equiv) and  $\text{Et}_3\text{N}$  (0.42 mL; 3.00 mmol; 2 equiv) in  $\text{CH}_3\text{CN}$  (10 mL) under a nitrogen atmosphere. After stirring at room temperature for 3 h the organic layer was washed with a saturated solution of  $\text{NaHCO}_3$  (3  $\times$  40 mL), dried over  $\text{MgSO}_4$ , and concentrated *in vacuo* to yield quantitatively compound **9** as a green foam.  $^1\text{H}$  NMR ( $\text{CDCl}_3$ ): 8.59 (d,  $J = 8.5$  Hz, 1H), 8.36 (d,  $J = 5.9$  Hz, 1H), 8.27 (dd,  $J = 7.3$  Hz,  $J = 1.2$  Hz, 1H), 7.60 (m, 2H), 7.24 (d,  $J = 7.5$  Hz, 1H), 5.55 (bs, 1H,  $\text{NH}$ ), 5.09 (bs, 1H,  $\text{NH}$ ), 3.41 (m, 10H), 3.16 (m, 2H), 1.48 (s, 9H).  $^{13}\text{C}$  NMR ( $\text{CDCl}_3$ ): 159.6, 135.9, 131.2, 130.7, 130.5, 130.2, 129.2, 124.1, 119.8, 116.1, 80.2, 78.2, 71.1, 71.1, 70.9, 70.1, 46.3; 43.9, 41.1, 29.3. MS:  $[\text{M} + \text{H}]^+$ : 482.23

**N-[8-(1-(Dimethylamino)-5-naphthalenesulfonamide)-3,6-dioxaoctyl]-3,5-dimaleimidyl-1-benzamide (10):** Under a nitrogen atmosphere at room temperature were combined amide **9** (429 mg; 0.89 mmol; 1 equiv) and trifluoroacetic acid (10 mL). The reaction was stirred for 3 h and concentrated *in vacuo* to afford the corresponding amine quantitatively as its trifluoroacetate salt, used immediately in the following step. To a solution of acyl chloride **3** (323 mg; 0.98 mmol; 1.1 equiv) in dry  $\text{CH}_2\text{Cl}_2$  (20 mL) was added the amine (543 mg; 0.89 mmol; 1 equiv) in  $\text{CH}_2\text{Cl}_2$  followed by  $\text{Et}_3\text{N}$  (0.62 mL; 4.46 mmol; 5 equiv) under a nitrogen atmosphere and stirred at room temperature overnight. The organic layer was washed with a saturated solution of  $\text{NaHCO}_3$  (2  $\times$  30 mL) dried over  $\text{MgSO}_4$  and concentrated *in vacuo*. The crude product was purified by precipitation in  $\text{CH}_2\text{Cl}_2$ – $\text{Et}_2\text{O}$ . The resulting solid was filtered and washed with  $\text{Et}_2\text{O}$  to give the compound **10** as a beige solid in 44% yield. Mp: 118–120 °C.  $^1\text{H}$  NMR ( $\text{CDCl}_3$ ): 8.54 (d,  $J = 8.6$  Hz, 1H), 8.30 (d,  $J = 8.6$  Hz, 1H), 8.22 (d,  $J = 7.3$  Hz, 1H), 7.94 (d,  $J = 1.8$  Hz, 2H), 7.67–7.46 (m, 5H), 7.30 (bs, 1H,  $\text{NH}$ ), 7.18 (d,  $J = 7.5$  Hz, 1H), 6.84 (s, 4H), 5.99 (t,  $J = 5.8$  Hz, 1H,  $\text{NH}$ ), 3.63–3.41 (m, 10H), 3.14–3.10 (m, 2H), 2.89 (s, 6H).  $^{13}\text{C}$  NMR ( $\text{CDCl}_3$ ): 168.8, 165.5, 151.7, 136.2, 135.2, 134.2, 132.1, 130.2, 129.7, 129.5, 129.0, 128.1, 126.6, 125.3, 123.7, 123.1, 118.9, 115.1, 70.1, 69.7, 69.2, 45.3, 42.8, 39.9. MS:  $[\text{M} + \text{H}]^+$ : 676.21.

**N-[2-(1-(Dimethylamino)-5-naphthalene-sulfonyl)aminoethyl]-3-[3-(2-carboxy)ethylthio succinimidyl]-5-maleimidyl-1-benzamide (11):** A solution of mercaptopropionic acid (6.10  $\mu\text{L}$ ; 0.07 mmol; 1 equiv) in  $\text{CH}_3\text{CN}$  (3 mL) was added dropwise to **8** (410.3 mg; 0.70 mmol; 10 equiv) dissolved in a  $\text{CH}_3\text{CN}$ –DMSO (1:1, v/v, 20 mL) solution. The resulting reaction mixture was stirred at room temperature overnight. The  $\text{CH}_3\text{CN}$  was removed *in vacuo*, and  $\text{Et}_2\text{O}$  (20 mL) was added to the mixture to precipitate **11** and the excess of **8**. The DMSO was removed by filtration, and the resulting residue was triturated with MeOH (20 mL). After filtration the MeOH was concentrated *in vacuo* to afford the desired compound **11** (40 mg; 0.07 mmol; 82%) as a yellow solid. Mp: 155–157 °C.  $^1\text{H}$  NMR ( $\text{CDCl}_3$ ): 8.32 (d,  $J = 8.3$  Hz, 1H), 8.21–8.19 (m, 1H), 8.06–7.98 (m, 2H), 7.76 (s, 2H), 7.34–7.30 (m, 4H), 6.92 (d,  $J = 7.5$  Hz; 1H), 6.72 (s, 2H), 3.31 (bs, 2H), 2.96–2.93 (m, 6H), 2.71–2.63 (m, 2H), 2.67 (s, 6H).  $^{13}\text{C}$  NMR ( $\text{CDCl}_3$ ): 168.9, 165.5, 135.7, 135.5, 134.8, 134.3, 131.8, 130.0, 129.5, 129.3, 128.9, 128.0, 125.6, 124.1, 123.0, 119.0, 115.0, 77.4, 45.8, 45.2, 42.6, 39.9, 34.3, 26.7. MS:  $[\text{M} + \text{H}]^+$ : 694.16.

**N-[2-(1-(Dimethylamino)-5-naphthalene-sulfonyl)aminoethyl]-3,5-di[3-(2-carboxy)ethyl thiosuccinimidyl]-1-benzamide (12):** Com-

pound **8** (125 mg; 0.21 mmol; 1 equiv) was dissolved in a DMSO–DMF solution (5:1, v/v, 50 mL). Mercaptopropionic acid (46.2  $\mu$ L; 0.53 mmol; 2.5 equiv) was added, and the mixture was stirred at room temperature for 72 h. Distilled water (50 mL) and  $\text{CHCl}_3$  (75 mL) were added, and the organic layer was washed with  $\text{H}_2\text{O}$  ( $2 \times 40$  mL), dried over  $\text{MgSO}_4$ , filtered, and concentrated *in vacuo* to afford **12** (125 mg; 0.213 mmol; 63%) as a yellow solid. Mp: 87–89 °C.  $^1\text{H}$  NMR (acetone- $d_6$ ): 8.52 (d,  $J = 8.5$  Hz, 1H), 8.33 (d,  $J = 8.6$  Hz, 1H), 8.25 (m, 1H, NH), 8.20 (d,  $J = 7.3$  Hz, 1H), 7.82 (d,  $J = 1.7$  Hz, 2H), 7.62–7.48 (m, 3H), 7.20 (d,  $J = 7.5$  Hz, 1H), 4.23 (dd,  $J = 9.2$  Hz,  $J = 4.1$  Hz, 2H), 3.47–3.42 (m, 4H), 3.17–2.96 (m, 8H), 2.83 (s, 6H), 2.76–2.70 (m, 4H).  $^{13}\text{C}$  NMR (acetone- $d_6$ ): 176.6, 174.6, 173.5, 152.7, 136.6, 134.0, 130.7, 130.6, 130.4, 129.7, 128.9, 128.7, 126.4, 124.1, 120.0, 116.0, 45.5, 43.2, 40.8, 40.6, 36.9, 30.1. MS:  $[\text{M} + \text{H}]^+$ : 800.17.

**N-[8-(1-(dimethylamino)-5-naphthalenesulfonamide)-3,6-dioxoac-tan-1-yl]-3,5-di[3-(2-carboxy)ethyl]thiosuccinimidyl]-1-benzamide (13):** To a solution of **10** (100 mg; 0.15 mmol; 1 equiv) in  $\text{CHCl}_3$  (10 mL) was added the mercaptopropionic acid (32  $\mu$ L; 0.37 mmol; 2.5 equiv). After the mixture was stirred at room temperature for 23 h,  $\text{Et}_2\text{O}$  (10 mL) was added to the mixture. The resulting white precipitate was filtered and washed with  $\text{Et}_2\text{O}$  ( $2 \times 5$  mL) to afford **13** as a white powder (105 mg; 0.12 mmol; 79%). Mp: 122–124 °C.  $^1\text{H}$  NMR (DMSO- $d_6$ ): 8.57 (m, 1H, NH), 8.33 (d,  $J = 8.2$  Hz, 1H), 8.18 (d,  $J = 8.7$  Hz, 1H), 8.01 (d,  $J = 6.8$  Hz, 1H), 7.77 (d,  $J = 1.5$  Hz, 2H), 7.51–7.39 (m, 2H), 7.33 (s, 1H), 7.10 (d,  $J = 7.3$  Hz, 1H), 4.02 (dd,  $J = 8.8$  Hz,  $J = 3.6$  Hz, 2H), 3.37–3.16 (m, 18H), 3.01–2.91 (m, 2H), 2.86–2.77 (m, 6H), 2.57–2.50 (m, 6H).  $^{13}\text{C}$  NMR (DMSO- $d_6$ ): 174.3, 172.5, 172.2, 163.9, 150.6, 135.0, 131.6, 128.7, 128.5, 128.4, 127.4, 126.8, 126.5, 124.8, 122.2, 118.3, 114.0, 68.9, 68.8, 68.2, 44.3, 41.5, 35.2, 33.4, 25.9. MS:  $[\text{M} + \text{H}]^+$ : 888.22.

**N-[2-tert-Butoxycarbonylaminoethyl]-3-[3-(2-carboxy)ethylthio-succinimidyl]-5-maleimidyl-1-benzamide (14):** Mercaptopropionic acid (58.0  $\mu$ L; 0.66 mmol; 1 equiv) in  $\text{CHCl}_3$  (10 mL) was added to a solution of compound **6** (300 mg; 0.66 mmol; 1 equiv) in  $\text{CHCl}_3$  (100 mL). The mixture was stirred at room temperature for 4 h, and the solvent was removed *in vacuo*. The crude product was purified on a silica preparative TLC plate (2 mm thickness; (EtOAc–Hex–AcOH, 7:3:0.5, v/v)), leading to **14** as a pink solid (16 mg; 0.03 mmol; 4.3%). Mp: 67–69 °C.  $^1\text{H}$  NMR (acetone- $d_6$ ): 8.00 (s, 1H), 7.81 (s, 1H), 7.63 (s, 1H), 7.03 (s, 2H), 4.14 (dd,  $J = 9.2$  Hz,  $J = 3.9$  Hz, 1H), 3.52–3.46 (m, 4H), 3.33–3.30 (m, 2H), 2.77–2.73 (m, 4H), 1.31 (s, 9H).  $^{13}\text{C}$  NMR (acetone- $d_6$ ): 170.1, 135.5, 131.8, 128.0, 125.8, 125.6, 78.9, 40.8, 40.7, 37.0, 28.6, 27.5. MS:  $[\text{M} + \text{Na}]^+$ : 583.15.

**N-[2-tert-Butoxycarbonylaminoethyl]-3,5-di[3-(2-carboxy)ethylthio-succinimidyl]-1-benzamide (15):** Mercaptopropionic acid (0.15 mL; 1.75 mmol; 2.5 equiv) was added to a solution of compound **6** (317 mg; 0.70 mmol; 1 equiv) in  $\text{CHCl}_3$  (25 mL). The mixture was stirred at room temperature for 20 h, and the solvent was removed *in vacuo*. The resulting black oil was triturated with  $\text{Et}_2\text{O}$  and filtered to afford quantitatively **15** as a beige powder. Mp: >180 °C.  $^1\text{H}$  NMR (acetone- $d_6$ ): 8.18 (bs, 1H, NH), 7.91 (d,  $J = 1.8$  Hz, 2H), 7.47 (bs, 1H), 6.29 (bs, 1H, NH), 4.25 (dd,  $J = 9.2$  Hz,  $J = 4.1$  Hz, 2H), 3.53–3.47 (m, 4H), 3.34–3.20 (m, 7H), 3.10–3.06 (m, 2H), 2.78–2.71 (m, 5H), 1.40 (s, 9H).  $^{13}\text{C}$  NMR (acetone- $d_6$ ): 176.4, 174.3, 173.1, 165.7, 157.1, 137.1, 134.0, 128.6, 126.3, 78.9, 41.2, 40.8, 40.7, 37.0, 34.6, 28.6, 27.5. MS:  $[\text{M} + \text{Na}]^+$ : 689.16.

**Spectroscopic Measurements.** Absorption measurements were done on a Cary-100 spectrometer and fluorescence studies were carried out on a Cary Eclipse and an Edinburgh Instruments FLS-920 fluorometer after deaerating the samples thoroughly with nitrogen for 20 min. Fluorescence quantum yields were measured at  $10^{-5}$  M by exciting the corresponding compounds that were optically matched at 335 nm in spectroscopic grade acetonitrile and compared to dansylamide ( $\phi_{511}$  nm = 0.37<sup>22</sup>) excited at the same wavelength.<sup>23</sup> The actinometer absorbencies, and those of the compounds, were matched at the excitation wavelength to within 5%. The phosphorescence measure-

ments were done in a 1:4 methanol/ethanol glass matrix at 77 K, exciting at the compound's absorption maximum. The fluorescence lifetimes were obtained via an Edinburgh Instruments time-resolved FLS-920 fluorometer. The samples for lifetime measurements were prepared at  $10^{-5}$  M in anhydrous acetonitrile and were thoroughly deaerated with nitrogen prior to analysis. The lifetime decays (dansylamide = 14.6 ns; **12** = 14.0 ns; **13** = 17.1 ns) were fitted with a signal variable monoexponential decay leading to  $\geq 99\%$  correlation factors. Stern–Volmer fluorescence quenching was done according to the following standard protocol: Fluorophore **1** was dissolved in anhydrous and deaerated acetonitrile, and its emission spectrum was recorded by exciting at  $\lambda = 335$  nm. Known amounts of a deaerated stock solution of quencher were added to the fluorophore sample. The resulting fluorescence decrease was recorded and compared to the unquenched fluorescence. Extreme care was taken to ensure the absorbance of the quencher was below 5% of the fluorophore absorbance at the excitation wavelength used for the measurements. The Stern–Volmer quenching constant ( $K_{SV}$ ) was taken from the linear portion of the slope of relative fluorescence change as a function of the quenching concentration. The change in the fluorophore's fluorescence lifetime with various maleimide quenchers was studied in a similar manner to afford the Stern–Volmer constants. The subsequent dynamic quenching rate constants ( $k_q$ ) for the fluorophore fluorescence deactivation with the various maleimide quenchers were calculated by dividing the measured values of  $K_{SV}$  by the fluorescence lifetime of **1**.

The triplet–triplet transient absorption spectrum was measured in anhydrous acetonitrile using a Luzchem mini-LFP system excited at 355 nm with the third harmonic from a Continuum YAG:Nd Sure-lite laser. The triplet quantum yields were measured by optically matching samples within 5% at 355 nm relative to anthracene. The anthracene triplet was monitored at 420 nm.<sup>24,25</sup>

**Electrochemical Measurements.** Cyclic voltammetric measurements were performed on a Bio Analytical Systems EC Epsilon potentiostat with a scan rate of 100 mV/s. The compounds were dissolved in anhydrous and deaerated acetonitrile at  $10^{-5}$  M along with the addition of 0.1 M  $\text{NBu}_4\text{PF}_6$ . The redox potentials were measured after deaerating the solution with nitrogen for 20 min. A glassy carbon electrode and a platinum electrode were employed as working and auxiliary electrodes, respectively. A saturated Ag/AgCl electrode was used as the reference electrode.<sup>26</sup>

## Results and Discussion

**Synthesis.** The convergent synthetic routes shown in Scheme 1 allowed the efficient preparation of all compounds by straightforward procedures, involving typical protection/coupling/deprotection strategies. The maleimide groups of compound **2** were introduced according to the typical two-step transformation procedure<sup>10,18,27</sup> in excellent yield. The activation of benzoic acid derivative **2**, prior to amide coupling, was effected efficiently through the preparation<sup>28</sup> of acid chloride **3**, as a stable synthetic intermediate in quantitative yield.

Dimaleimide fluorogens **8** and **10** were prepared by slightly different routes, as shown in Scheme 1. First of all, commercially available diamines were monoprotected as Boc derivatives **4** and **5** in excellent yield by adding a 10-fold excess of diamine to Boc anhydride. The condensation of **3** with amine **4** according to a literature procedure<sup>29</sup> gave amide **6** in excellent yield, which

(22) Li, Y.-H.; Chan, L.-M.; Tyer, L.; Moody, R. T.; Himel, C. M.; Hercules, D. M. *J. Am. Chem. Soc.* **1975**, *97*, 3118.

(23) Demas, J. N.; Crosby, G. A. *J. Phys. Chem.* **1971**, *75*, 991.

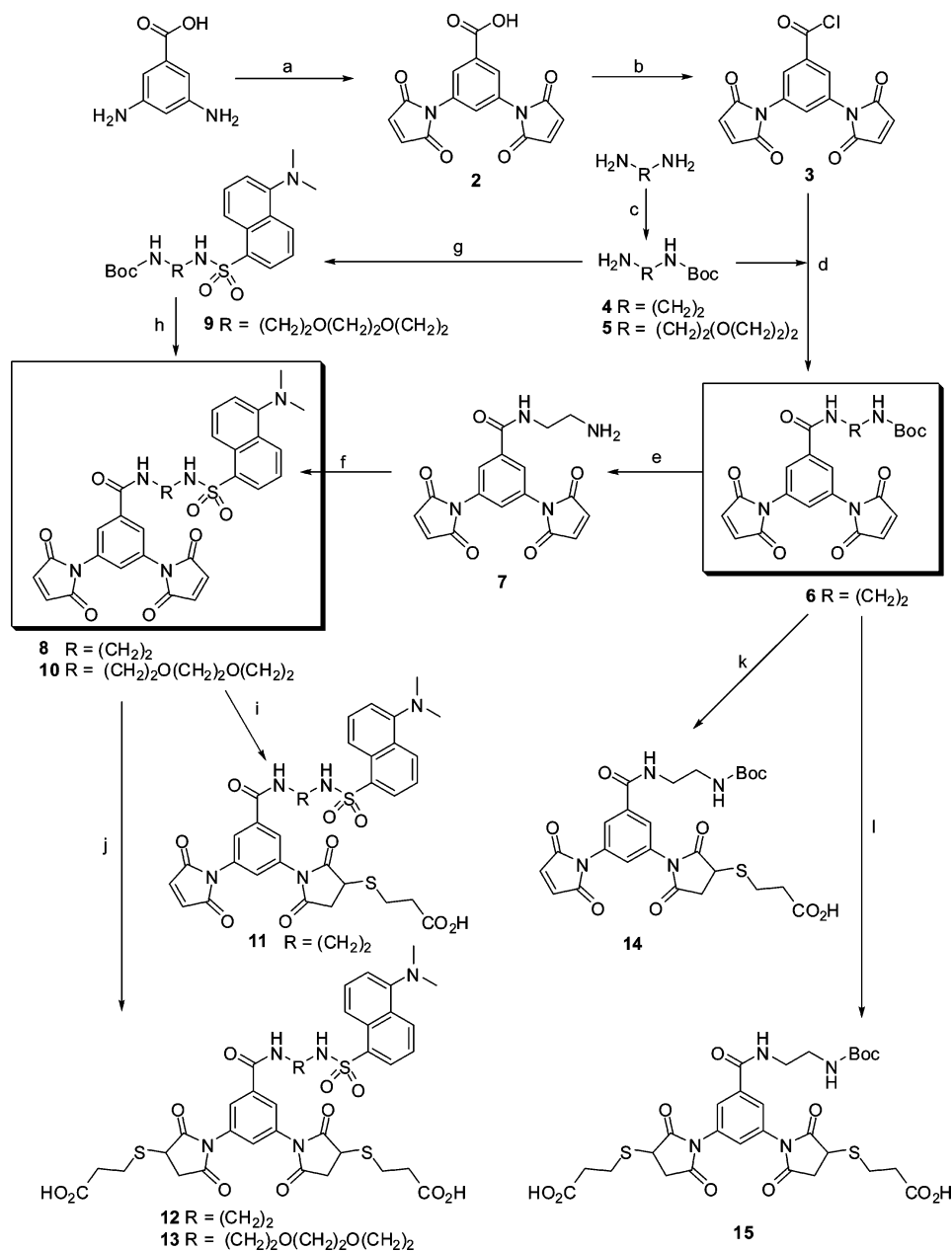
(24) Scaiano, J. C. *CRC Handbook of Organic Photochemistry*; CRC Press: Boca Raton, FL, 1989.

(25) Carmichael, I.; Hug, G. L. *J. Phys. Chem. Ref. Data* **1986**, *15*, 1.

(26) Connelly, N. G.; Geiger, W. E. *Chem. Rev.* **1996**, *96*, 877.

(27) Reddy, P. Y.; Kondo, S.; Fujita, S.; Toru, T. *Synthesis* **1998**, 999.

(28) Pickaert, G.; Cesario, M.; Ziessel, R. *J. Org. Chem.* **2004**, *69*, 5335.

Scheme 1<sup>a</sup>

<sup>a</sup> (a) (i) Maleic anhydride, CHCl<sub>3</sub>, reflux 20 h, (ii) Ac<sub>2</sub>O, NaOAc, 100 °C, 1.5 h, 72% for two steps; (b) SOCl<sub>2</sub>, reflux, 3.5 h, 98%; (c) Boc<sub>2</sub>O, CH<sub>2</sub>Cl<sub>2</sub>, rt, 16 h, 89%; (d) **4**, NEt<sub>3</sub>, CH<sub>2</sub>Cl<sub>2</sub>, rt, 3 h, 96%; (e) TFA, rt, 1.5 h, 100%; (f) dansyl chloride, NEt<sub>3</sub>, CH<sub>3</sub>CN, rt, 24 h, 78%; (g) **5**, dansyl chloride, NEt<sub>3</sub>, CH<sub>2</sub>Cl<sub>2</sub>, rt, 3 h, 100%; (h) (i) TFA, rt, 1.5 h, (ii) **3**, NEt<sub>3</sub>, CH<sub>2</sub>Cl<sub>2</sub>, 24 h, 44% for two steps; (i) 3-mercaptopropionic acid, CH<sub>3</sub>CN/DMSO, rt, 24 h, 82%; (j) **12**: mercaptopropionic acid, DMSO/DMF, rt, 72 h, 63%; **13**: mercaptopropionic acid, CHCl<sub>3</sub>, rt, 24 h, 79%; (k) mercaptopropionic acid, CHCl<sub>3</sub>, rt, 4 h, 4.3%; (l) mercaptopropionic acid, CHCl<sub>3</sub>, rt, 20 h, 100%.

was subsequently deprotected<sup>30</sup> to give primary amine **7**, quantitatively. This amine was then coupled with commercially available dansyl chloride to give the desired fluorogen **8** in excellent yield. For fluorogen **10**, the relative order of addition of the dimaleimide benzoyl moiety and dansyl chloride to the diamine was inverted with respect to the synthesis of fluorogen **8**. This was judged to be necessary to avoid potential degradation of the maleimide groups in the presence of the very nucleophilic PEG-diamine **5**. For this reason, PEG-diamine **5** was first coupled with dansyl chloride to give amide **9**, quantitatively.

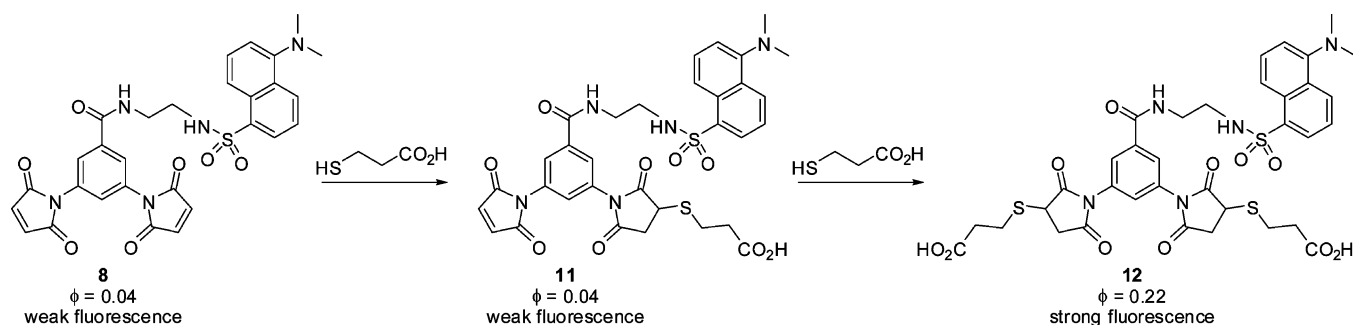
Removal of the Boc group<sup>30</sup> from **9** followed by immediate reaction of the resulting primary amine with acid chloride **3** afforded fluorogen **10** in moderate yield for the two steps.

The design of the synthetic route shown in Scheme 1 allows dimaleimide fluorogens to be prepared simply, rapidly, and in parallel. Furthermore, the alternate use of different activated fluorophores, diaminobenzoic acid derivatives, or diamine linkers permit, with relative ease, the facile variation of the color of fluorophore, the distance between the maleimide groups, or the nature of the spacer of the final fluorogen. These advantages will be exploited in forthcoming work.

**Fluorescence.** Shown in Table 1 are the quantum yields measured for reference compounds dansylamide and **1**, for

(29) Hidai, Y.; Kan, T.; Fukuyama, T. *Chem. Pharm. Bull.* **2000**, *48*, 1570.  
 (30) Jasys, V. J.; Kelbaugh, P. R.; Nason, D. M.; Phillips, D.; Rosnack, K. J.; Saccamano, N. A.; Stroh, J. G.; Volkmann, R. A. *J. Am. Chem. Soc.* **1990**, *112*, 6696.

Scheme 2

**Table 1.** Molar Absorption Coefficients and Fluorescence Quantum Yields Measured in Acetonitrile at  $\lambda_{\text{exc}} = 335$  nm

compound	$\epsilon_{\text{max}}^a$ (M <sup>-1</sup> cm <sup>-1</sup> )	$\lambda_{\text{em}}$ (nm)	$\phi_{\text{fl}}^b$
dansylamide	3200	511	0.37 <sup>c</sup>
<b>1</b>	3200	511	0.35
<b>8</b>	3700	511	0.04
<b>10</b>	3800	525	0.03
<b>11</b>	2700	458	0.04
<b>12</b>	2700	511	0.22
<b>13</b>	3000	525	0.11

<sup>a</sup> Measured at 335 nm. <sup>b</sup> Quantum yields were calculated according to the method shown in ref 23. <sup>c</sup> Value taken from ref 22.

dimaleimide dansyl derivatives **8** and **10**, and for their respective dithiol adducts **12** and **13**. Comparison of the quantum yields of **8** and **10** to those of dansylamide and **1** shows the effect of an intramolecular dimaleimide moiety. Fluorescence efficiency is decreased by an order of magnitude, similar to what we observed previously, for naphthalene and coumarin derivatives bearing two maleimide groups attached directly to their fluorescent cores.<sup>18</sup> This quenching effect is of the same magnitude as that measured for various fluorophores attached to a single maleimide group, either directly or via an alkyl tether.<sup>11–14</sup> Compound **1** was prepared to verify that the quench effect observed in **8** and **10** was not due to conformational constraints introduced by alkyl substitution on the dansylamide nitrogen. The similarity of its quantum yield to that of the standard dansylamide clearly shows that it is not simply the alkylation of the dansylamide moiety of **8** and **10** that leads to their quenched fluorescence, but rather the presence of at least one maleimide group. Comparison of the quantum yields of **8** and **10** to those of their dithiol adducts **12** and **13** confirm that fluorescence is restored to nearly the same efficiency as in the standard compounds.

Previously, we suggested that the reaction of only one maleimide group of a dimaleimide fluorogen is not sufficient to restore its latent fluorescence.<sup>16–18</sup> That is, only the dithiolated adduct fluoresces strongly, after *both* maleimide groups have undergone a thiol addition reaction. To verify this, authentic monothiolated adduct **11** was synthesized and purified. Comparison of its quantum yields with that of **8** and **12** confirms that the monothiolated derivative fluoresces as weakly as the quenched dimaleimide derivative. All restoration of fluorescence is realized upon reaction of the final maleimide group (Scheme 2). The successful design of future dimaleimide labeling agents will depend upon our understanding of the reactivity of the maleimide group (to be reported shortly) and the nature of its quench mechanism (*vide infra*).

**Table 2.** Relative Fluorescence in a 1:4 Methanol/Ethanol Glass Matrix at 77 K Compared to RT Solution,  $\lambda_{\text{exc}} = 335$  nm

compound	$\lambda_{\text{em}}(77\text{ K})$ (nm)	$\lambda_{\text{em}}(298\text{ K})$ (nm)	$\phi_{\text{fl}}(\text{rt})$	$\phi_{\text{fl}}(77\text{ K})$	$\phi_{\text{IC}}^b$
<b>1</b>	462	511	0.35	1.0	0.65
<b>6</b>	490	490	-	- <sup>a</sup>	-
<b>8</b>	462	511	0.04	0.20	0.16
<b>12</b>	462	511	0.22	0.77	0.53

<sup>a</sup> The emission measured at 77 K is 6.6-fold greater than that at rt; however no value for the  $\phi_{\text{fl}}(\text{rt})$  is known. <sup>b</sup> The values of  $\phi_{\text{IC}}$  were calculated according to:  $\phi_{\text{fl}} + \phi_{\text{ISC}} + \phi_{\text{IC}} \approx 1$ , where  $\phi_{\text{ISC}} = 0$  determined by LFP and  $\phi_{\text{fl}}(77\text{ K}) - \phi_{\text{fl}}(\text{rt}) \approx \phi_{\text{IC}}$ .

**Quenching Mechanism.** It is evident from Table 1 that the maleimide group efficiently quenches the dansylamide fluorophore excited state. Even though quenching of the fluorophore occurs in the presence of the maleimide, the mechanism by which this occurs is not clearly understood. Knowledge of the deactivation mechanism is therefore quintessential for the future design of new generations of fluorescent protein labels of this type.<sup>18</sup> There are three plausible types of quenching modes available for dansylamide deactivation in the presence of the maleimide, these are: (1) Förster energy transfer, (2) Dexter energy transfer, and (3) photoinduced electron transfer (PET). To determine the type of fluorescence quenching, we first examined the fluorescence deactivation of dansylamide. This is of importance owing to the limited number of photophysical studies of this fluorophore and the characterization of its excited states.<sup>31–33</sup>

Given the complexity in assigning the quenching mechanism without knowing the deactivation modes of the native fluorophores, we first examined the fate of the excited state of dansylamide and **1**. There are generally three distinct pathways for the singlet deactivation for such fluorophores, namely, (1) fluorescence, (2) intersystem crossing (ISC), and (3) internal conversion (IC). The reported<sup>34,35</sup> low fluorescence quantum yield ( $\phi_{\text{fl}} = 0.35$ ) for dansylamide suggests that its deactivation occurs predominately by nonradiative means such as ISC or IC. Since the fluorophores studied herein are highly conjugated, ISC to the triplet state is highly probable owing to the narrowing of the singlet–triplet gap, which occurs with conjugated compounds. The triplet manifold is additionally expected to be populated by ISC occurring by slight spin orbit coupling induced

(31) Metivier, R.; Leray, I.; Valeur, B. *Photochem. Photobiol. Sci.* **2004**, *3*, 374.

(32) Hebbink, G. A.; Klink, S. I.; Grave, L.; Alink, P. G. B. O.; Veggel, F. C. J. M. v. *Chem. Phys. Chem.* **2002**, *3*, 1014.

(33) Holmes-Farley, S. R.; Whitesides, G. M. *Langmuir* **1986**, *2*, 266.

(34) Himel, C. M.; Mayer, R. T. *Anal. Chem.* **1970**, *42*, 130.

(35) Chen, R. F. *Nature* **1966**, *209*, 69.

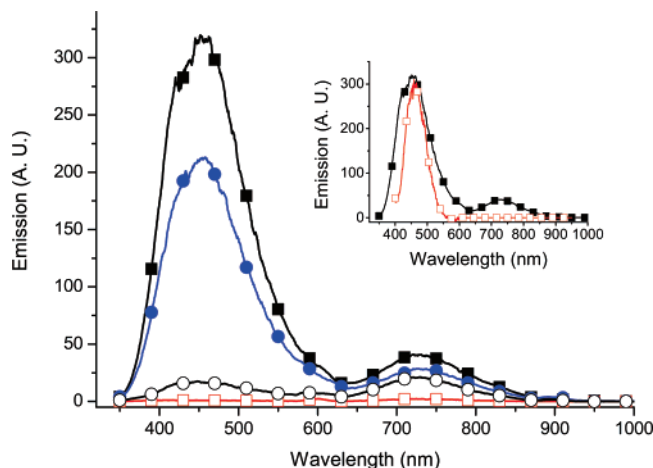


**Figure 1.** Relative phosphorescence spectra of **1** (■), **6** (○), **8** (□), dansylamide (●) recorded at 77 K in a 1:4 methanol/ethanol glass matrix. Inset: normalized fluorescence (open squares) measured at room temperature, and phosphorescence (closed squares) of **1** measured at 77 K in a 1:4 methanol/ethanol glass matrix.

by the heavy atom effect of the heteroatoms.<sup>36</sup> Evidence for the triplet state can be obtained from phosphorescence measurements at 77 K in a methanol/ethanol glass. Such measurements produced a new long wavelength emission around 720 nm that is consistent with the existence of a triplet state (Figure 1 and Table 2). There was no emission shift observed among **1** and **6** and **8**. This confirms the compounds have the same triplet energy and that there is no conjugation between the maleimides and the fluorophore. This notwithstanding, inconclusive evidence for the fluorescence quenching of dansylamide by ISC is obtained from the phosphorescence measurements because this low temperature artificially populates the triplet state such that its quantification is not possible. Alternatively, evidence for the manifold shift to the triplet state by ISC is possible via laser flash photolysis (LFP). The high degree of conjugation of dansylamide should provide an intense signal visible around 400 nm by LFP. This expected signal would be similar to anthracene and decay with similar first-order kinetics as those shown for anthracene in Figure 2. However, direct excitation of the fluorophore at 355 nm failed to produce any visible triplet within the time frame of the experiment. This provides undeniable proof that dansylamide and **1** do not undergo singlet deactivation by ISC. Furthermore, since Dexter energy transfer occurs mostly by the triplet manifold, this cannot be the mechanism responsible for efficient fluorophore quenching with maleimides.

Having ruled out ISC, the predominant method of dansylamide excited-state deactivation must therefore occur by the nonradiative route of IC according to the following energy conservation equation:  $\phi_{\text{fl}} + \phi_{\text{ISC}} + \phi_{\text{IC}} \approx 1$ . Evidence that the remaining 65% of the excited-state energy is dissipated by IC is derived from low-temperature fluorescence measurements. All normal modes of energy dissipation by bond rotation are suppressed at 77 K, resulting in a fluorescence increase if IC deactivation is present. Accurate values for the low-temperature fluorescence yields are difficult because of the experimental errors associated with calculating the weak fluorescence signal at room temperature relative to the intense one at 77 K.

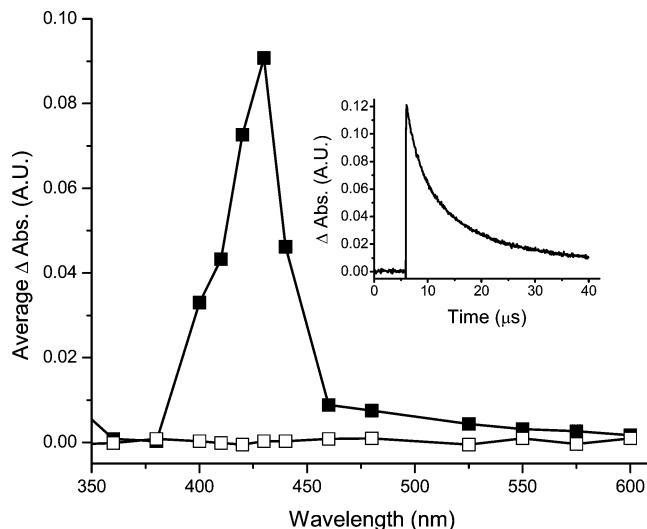


**Figure 2.** Transient absorption spectra recorded in acetonitrile, at 2.5 μs after the excitation pulse at 355 nm, of anthracene (■) and **1** (□). Inset: transient decay of anthracene monitored at 425 nm.

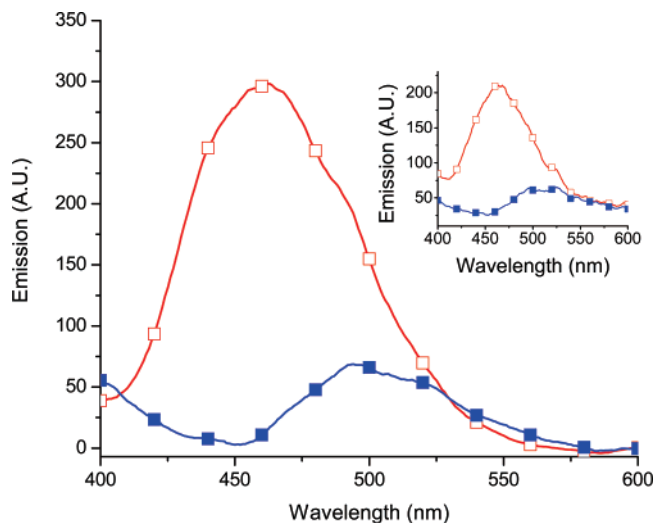


**Figure 3.** Relative fluorescence of **1** measured in a 1:4 methanol/ethanol matrix at rt (■) and 77 K (□). Inset: Relative fluorescence of **12** measured in a 1:4 methanol/ethanol matrix at rt (■) and 77 K (□).

Nonetheless, an approximately 4-fold fluorescence increase was observed at 77 K, relative to the room-temperature emission, for all compounds studied (Figure 3). This confirms that energy dissipation occurs predominantly by IC and is consistent with previous reports of similar dansylamides.<sup>37,38</sup> IC in the dansyl group is understood to occur by efficient deactivation involving bond rotation of the heteroatomic groups bound to the naphthalene ring and is consistent with other substituted fluorophores such as rhodamine and fluorescein.<sup>39</sup> The hypsochromically shifted emission observed at 77 K relative to room temperature is from the highest energy rotamer that is exclusively formed at this low temperature. The amount of IC for **1** can be calculated from the two temperature fluorescence measurements according to  $\phi_{\text{fl}}(77\text{ K}) - \phi_{\text{fl}}(\text{rt}) = \phi_{\text{IC}}$ . The same IC deactivation occurs for both **1** and **12**, which contains the maleimide covalently linked to the dansylamide fluorophore (inset of Figure 3).

(37) Chen, H.; Jiang, Y. B. *Chem. Phys. Lett.* **2000**, *325*, 605.

(38) Takehira, K.; Suzuki, K.; Hiratsuka, H.; Tobita, S. *Chem. Phys. Lett.* **2005**, *413*, 52.

(39) Perez Guarin, S. A.; Tsang, D.; Skene, W. G. *New J. Chem.* **2007**, *31*, 210.

(36) Turro, N. J. *Modern Molecular Photochemistry*; University Science Books: Sausalito, CA, 1991.

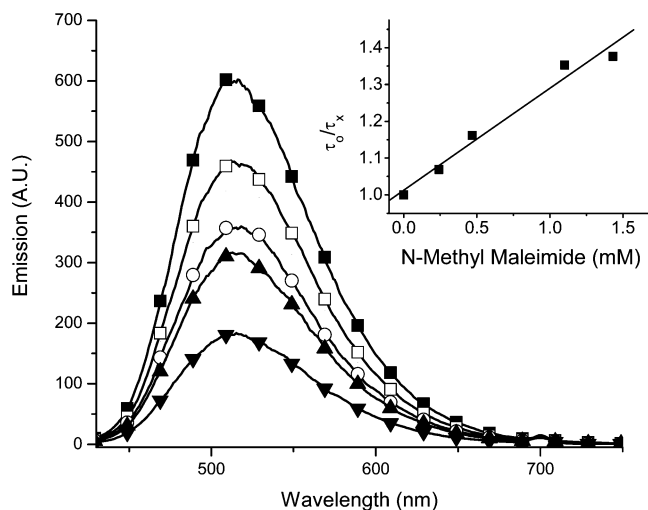


**Figure 4.** Fluorescence quenching of the singlet excited-state of **1** with varying amounts of *N*-methyl maleimide quencher, measured in deaerated acetonitrile: 0 mM (■), 0.24 mM (□), 0.47 mM (○), 1.1 mM (▲), 1.43 mM (▼). Inset: Stern–Volmer plot showing the relative fluorescence lifetime change without and with quencher as a function of *N*-methyl maleimide concentration.

The absence of a visible triplet by LPF implies deactivation of the fluorophore's singlet excited-state occurs preferentially from the singlet manifold. The mechanism of maleimide quenching must therefore occur from this manifold and can involve either Förster energy transfer or PET. Given the incompatibility of the maleimide absorption and the dansylamide emission spectral overlap, Förster quenching is not a viable mechanism. PET is therefore a feasible quenching mechanism.<sup>40</sup> To confirm electron-transfer deactivation, the Stern–Volmer quenching of **1** was investigated with various maleimides. This method examines either the decrease in steady-state fluorescence or fluorescence lifetimes with the addition of known amounts of quencher and provides information regarding quenching kinetics and ultimately the quenching mechanism. The typical fluorescence behavior observed for all quenchers studied herein is presented by the Stern–Volmer plot in Figure 4. The Stern–Volmer ( $K_{SV}$ ) quenching rate constants are derived from slopes of the quenching plots. The desired second-order quenching rate constant ( $k_q$ ) is calculated from  $K_{SV}$  by dividing by the fluorescence lifetime of **1** ( $\tau = 22.8$  ns), leading to  $k_q$ . The calculated values derived from the uniquely monoexponential lifetimes for *N*-methyl maleimide ( $1.2 \times 10^{10} \text{ M}^{-1} \text{ s}^{-1}$ ), **6** ( $8.5 \times 10^9 \text{ M}^{-1} \text{ s}^{-1}$ ), and **15** ( $2.0 \times 10^{10} \text{ M}^{-1} \text{ s}^{-1}$ ) are close to the diffusion limit in acetonitrile, which is consistent with a fast quenching process such as electron transfer. The time-resolved Stern–Volmer studies (inset Figure 4) further confirm the quenching process is dynamic. This dynamic quenching mechanism is further supported by the absence of any change in the absorption spectra when **1** and *N*-methyl maleimide are combined. Such a change would otherwise indicate the formation of a ground state complex leading to static quenching. The observed dynamic quenching implies the quencher must diffuse close to the fluorophore within the fluorescence lifetime of the dansylamide in order to deactivate the singlet excited state. Given that the quencher and the fluorophore are inherently confined in close proximity, the quencher rapidly deactivates

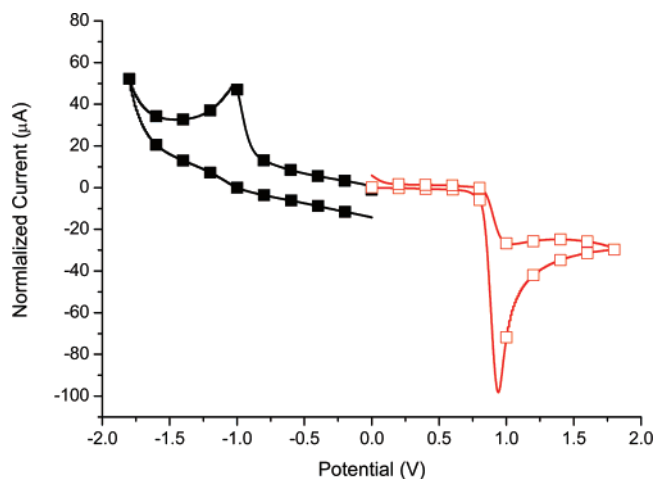


**Figure 5.** Cyclic voltammetry of **1** (□) and **6** (■), measured in anhydrous and deaerated dichloromethane, with  $\text{Bu}_4\text{NPF}_6$  as the supporting electrolyte and using a  $\text{Ag}/\text{Ag}^+$  reference electrode and a 100 mV/s scan speed.

the dansylamide via electron transfer. The effective quenching concentration for intramolecular quenching processes is 1 M while the average singlet excited-state concentration produced upon irradiation is ca.  $\mu\text{M}$ . Therefore, the maleimide quencher concentration is approximately 6 orders of magnitude greater than the dansylamide singlet excited-state concentration when the two groups are tethered together such as in **8**. This large concentration leads to rapid and efficient intramolecular electron-transfer quenching occurring in less than 100 ps.

Further evidence for electron-transfer quenching is derived from the complementarity of the electron donor and acceptor energy levels. The suitability of the dansylamide fluorophore donor and the maleimide acceptor to undergo photoinduced electron transfer is empirically calculated according to the Rehm–Weller equation:  $\Delta G_{\text{eT}}^\circ = E(D^+/D - A/A^-) - \Delta E(0,0) - wp$ .<sup>41</sup> This relationship takes into account the capacity of **1** to donate its electron ( $E_{\text{ox}}$ ), the capacity of the maleimide group to accept the transferred electron ( $E_{\text{red}}$ ), and the reorganization energy ( $wp$ ). The oxidation and reduction potentials of **1** and **6**, respectively, are therefore required to calculate the energetics and hence the probability of PET. The oxidation potential of **1** (0.94 V) and the reduction potential of **6** (−1.03 V) were consequently measured by cyclic voltammetry (Figure 5). The energy gap ( $\Delta E(0,0)$ ) between the ground and excited singlet states of **1** must also be taken into account since PET involves electron transfer from the excited state. The required value is calculated from the intercept of the normalized plot of the absorption and fluorescence spectra, according to Figure 6. The reorganization energy can be ignored since it is a mere 5.5 kJ/mol for acetonitrile and is a negligible amount compared to the other thermodynamic parameters. The calculated values confirm that the electron transfer is energetically favored ( $\Delta G_{\text{eT}} = -112$  kJ/mol) and supports the proposed PET quenching mechanism. The back electron transfer is, however, slightly more favorable (−187 kJ/mol) and prevents separation of the charged species. The steric confinement of the maleimide and the dansylamide further prevents any charged species from diffusing apart. Nonetheless, the complementarity of the donor and acceptor

(40) Ceroni, P.; Laghi, I.; Maestri, M.; Balzani, V.; Gestermann, S.; Gorka, M.; Vögtle, F. *New J. Chem.*, **2002**, *26*, 66.

(41) Gilbert, A.; Baggott, J. *Essentials of Molecular Photochemistry*; CRC Press: Boca Raton, FL, 1991.

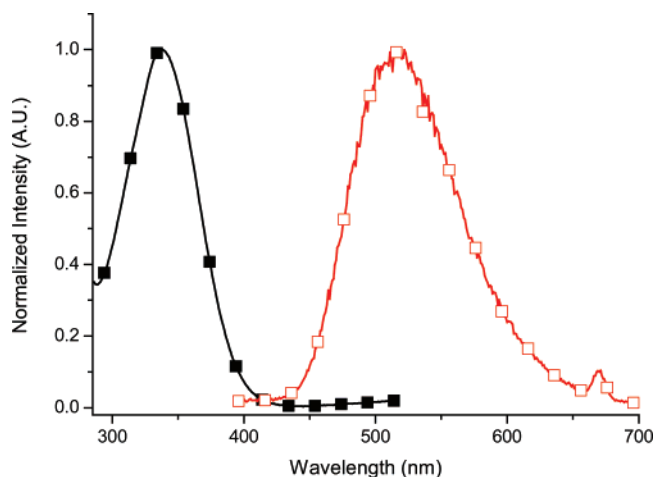


**Figure 6.** Normalized absorption (■) and fluorescence (□) of **1** in acetonitrile. The fluorescence spectrum was recorded in deaerated acetonitrile solution with  $\lambda_{\text{ex}} = 335$  nm.

redox potentials, together with the measured rapid  $k_q$ , provide sound evidence of dansylamide-maleimide quenching by a PET mechanism.

Recently, Maeda et al. studied the quench mechanism of maleimide groups attached to certain alkynyl pyrene derivatives designed as biomolecular probes.<sup>42</sup> Their Stern–Volmer study of pyrene fluorescence quenching by exogenous maleimide provided rate constants ( $k_q$ ) that were greater than diffusion controlled limits, leading them to propose a PET quenching mechanism. Specifically, they suggested that reduction of the maleimide group occurs by photoinduced oxidation from the excited pyrene. Herein, we propose a similar mechanism for the dansyl fluorophore, based on acceptable diffusion-controlled Stern–Volmer rate constants, supported by our LFP observations and unequivocally confirmed by our measured redox potentials.

These mechanistic conclusions have immediate consequences on the rational design of future fluorogenic labeling agents. For example, the efficiency of the PET-mediated quenching would be enhanced by using relatively rigid spacers between the fluorophore and dimaleimide moieties, whereas increasing the length of the spacer would reduce the PET efficiency. The PET mechanism is further evidenced by the similar photophysical results obtained from relatively short PEG and ethylene spacers for compounds **10** and **8**, respectively. Significantly different quenching rate constants would have been observed for these two compounds if a dynamic contact-type quenching mechanism was present. These two derivatives will ultimately further provide valuable insight into the mechanism with low-temperature studies and in viscous solvents. Furthermore, the PET quenching mechanism allows one to predict which fluorophores should be susceptible to maleimide quenching, owing to the

compatibility of their redox potentials and excited-state energies with those of maleimide, as predicted by the Rehm–Weller equation. For example, 7-methoxy coumarin<sup>43</sup> ( $E_{\text{ox}} = 1.84$  V;  $\Delta E(0,0) = 3.48$  eV), *F*-Bodipy<sup>44</sup> ( $E_{\text{ox}} = 0.95$  V,  $\Delta E(0,0) = 2.43$  eV) and Rhodamine B<sup>45</sup> ( $E_{\text{ox}} = 0.98$  V,  $\Delta E(0,0) = 2.23$  eV) are three fluorophores that span the emission spectrum from blue to red. Comparison of their standardized potentials against  $\text{Ag}/\text{Ag}^+$  (saturated) and spectroscopic properties with the reduction potential of maleimide suggests that while the quenching process would be highly efficient with the blue coumarin, it would be less efficient with the red rhodamine. Preliminary characterization of coumarin-<sup>18</sup> and rhodamine<sup>46</sup>-based fluorogens prepared in our laboratory confirms the predictive power of our mechanism. Given the popularity of maleimide-based fluorescent labeling techniques, the mechanistic conclusions of the photophysical study presented herein should prove to be broadly applicable as a predictive model in the rational design of future labeling agents.

## Conclusions

In conclusion, the establishment of a new, convergent synthetic route for the preparation of dimaleimide fluorogens permitted facile access to a large number of derivatives to be assessed as potential fluorescent protein labeling agents. In this study, dansyl fluorophore and dimaleimide quenchers were prepared and used to elucidate the mechanism of the dimaleimide quench phenomenon. The Stern–Volmer rate constants, lack of triplet formation, and the compatible redox potentials measured for the maleimides and for dansylamide herein provide the first unequivocal proof of a PET quench mechanism for the dimaleimide dansyl system, as was recently proposed for an analogous monomaleimide pyrene system.<sup>42</sup> Knowledge of this quenching mechanism will impact the design of future fluorogenic protein labeling agents. The ensuing predictive model will be tested, and the application of the resulting compounds to protein labeling will be reported in successive work.

**Acknowledgment.** The authors thank Stéphane Girouard, Christophe Loup, and Isabelle Roy (Keillor group) for their initial efforts on this project and Marie Bourgeaux and Sergio Perez (Skene group) for their generous technical assistance. This work was financially supported by the Canadian Institutes of Health Research (CIHR), the Natural Sciences and Engineering Research Council of Canada (NSERC), the University of Montreal Centre for Self-Assembled Chemical Structures (CSACS), and through additional equipment funding from the Canada Foundation for Innovation (CFI). K.C. is also grateful to NSERC for an Undergraduate Student Research Award.

JA0738125

(43) Seidel, C. A. M.; Schulz, A.; Sauer, M. H. M. *J. Phys. Chem.* **1996**, *100*, 5541.

(44) Goze, C.; Ulrich, G.; Ziesel, R. *J. Org. Chem.* **2007**, *72*, 313.

(45) Austin, J. M.; Harrison, I. R.; Quickenden, T. I. *J. Phys. Chem.* **1986**, *90*, 1839.

(46) Guy, J.; Keillor, J. W. Unpublished observations.

(42) Maeda, H.; Maeda, T.; Mizuno, K.; Fujimoto, K.; Shimizu, H.; Inouye, M. *Chem.–Eur. J.* **2006**, *12*, 824.